

# ADSORPTION OF CR (VI) BY CELLULOSE ADSORBENT PREPARED USING IONIC LIQUID AS A GREEN HOMOGENEOUS REACTION MEDIUM

YAN HAO,\* ZHENPENG CUI,\*\* HUI YANG,\* GUIBAO GUO,\* JINYAN LIU,\* ZHIXIANG WANG,\*  
ARIANE DENISET-BESSEAU\*\* and SAMY REMITA\*\*,\*\*

\**Institute of Applied Chemistry School of Chemistry and Chemical Engineering, Inner Mongolia University of Science and Technology, 7 Arden Str., 014010, Baotou, P.R. China*

\*\**Laboratory of Physical Chemistry, LCP, UMR 8000, CNRS, Paris-Saclay University, Campus d'Orsay, 15 Jean Perrin Av., 91405 Orsay Cedex, France*

\*\*\**CASER, SITI, National Conservatory of Arts and Crafts, CNAM, 292 Saint-Martin Str., 75141 Paris Cedex 03, France*

✉ *Corresponding authors: Yan Hao, haoyannk@163.com  
Samy Remita, samy.remita@u-psud.fr*

*Received March 22, 2017*

A cellulose-based adsorbent was originally prepared in ionic liquid and used for Cr (VI) ion removal. The preparation methodology involved chemical induced grafting of styrene onto microcrystalline cellulose (MCC), followed by chloroacetylation, amination and protonation processes in 1-butyl-3-methylimidazolium chloride ([Bmim]Cl) ionic liquid used as solvent. The shape and size of the adsorbents could be easily adjusted according to the requirements of wastewater treatment. FTIR and AFM-IR characterization methods demonstrated that grafting and copolymerization of styrene occurred on the surface of the MCC substrates. The grafting yield could be readily controlled by varying the experimental conditions, such as monomer concentration, reaction time and temperature. Besides, the adsorption of Cr (VI) ions onto the as-prepared cellulose-based adsorbent was investigated as a function of contact time and pH. The kinetic study revealed that adsorption could be achieved within 30 min. Also, the adsorption behavior of the prepared adsorbent was described by the Langmuir model.

**Keywords:** microcrystalline cellulose (MCC), ionic liquids (ILs), homogeneous phase graft copolymer, metal ion adsorbent

## INTRODUCTION

Today, water pollution, one of the most important life threatening problems of our world, is seriously threatening modern society.<sup>1</sup> Among the various contaminants of water, heavy metal pollution is a severe menace to aquatic ecosystems because a lot of these metals are potentially toxic, even at very low concentrations. Heavy metal ions are difficult to eliminate because they can only be transformed from one state to another rather than degraded by microbes.<sup>2</sup> The removal of heavy metal ions has become an urgent issue as they not only lead to direct and indirect risks to human health, but also disserve the whole ecosystem. Chromium is a typical heavy metal that has been used extensively

in industries, such as electroplating, metal finishing, pigments and leather tanning. Hexavalent chromium, Cr (VI) is known to be hazardous to the human body and can be absorbed through the digestive tract, skin and mucosa.<sup>3-5</sup> The drinking water guideline recommended by the Environmental Protection Agency (EPA) in the US is 100  $\mu\text{g L}^{-1}$ . Because of its highly toxic nature to biological systems, the removal of Cr (VI) from wastewater has attracted immense attention. Many kinds of treatment techniques have been employed to remove Cr (VI) from wastewater, for instance ion-exchange, reverse osmosis, precipitation, filtration, coagulation, electrolytic recovery and others.<sup>6,7</sup> Among all

these methods, adsorption is the most economically attractive and feasible due to its easy operation and the possibility to develop various cheap adsorbents.

Generally, adsorbents can be prepared by modifying various substrates, such as polyethylene (PE), polypropylene (PPE) through monomer grafting. However, these substrates may cause serious pollution to the environment because of their hard decomposition.<sup>8,9</sup> Therefore, it is of great significance to develop adsorptive composites from biopolymers for the removal of heavy metal pollutants from water. Among various biopolymers, cellulose is regarded as an environmentally friendly biomaterial suitable for synthesizing adsorbents, owing to its attractive properties, such as biodegradation, renewability and biocompatibility.<sup>10,11</sup> However, the heavy metal ions adsorption capacity of unmodified cellulose is very low, because of the limited functional groups in cellulose. Chemical modifications, such as densification, grafting copolymerization, crosslinking, amination and ethylation, have been used to overcome these drawbacks of cellulose. Among all the above methods, grafting copolymerization can provide new properties, such as a hydrophilic and hydrophobic nature, improved adsorption and ion exchange capacity of natural cellulose. Hajeeth *et al.* studied the graft copolymerization of acrylic acid with cellulose using ceric ammonium nitrate as redox initiator. The resultant adsorbent was used for the removal of Cr (VI) from aqueous solution, and adsorption process fitted well the Freundlich isotherm and followed pseudo-second-order kinetics.<sup>12</sup> Navarro *et al.* synthesized a new adsorbent by introducing polyethyleneimine (PEI) into porous cellulose carriers. Batch adsorption tests showed the ability of cellulose-PEI to selectively remove Hg (II) even in acidic regions.<sup>13</sup>

The insolubility of cellulose has become a bottleneck for its application. Since cellulose is nearly insoluble in water and most organic solvents, modification of cellulose is mainly carried out in heterogeneous, non-green solvent systems. However, a major problem with heterogeneous systems is the unequal accessibility between the OH groups in the amorphous regions and those in the crystalline regions, leading to inhomogeneous substitution.<sup>14</sup> In addition, the heterogeneous reaction and non-green solvents also present limitations in terms of volatility,

toxicity and instability in processing.<sup>15</sup> Sun synthesized the amino-functionalized magnetic composite of cellulose that was able to remove Cr (VI).<sup>16</sup> The above preparation was carried out in NaOH/urea aqueous solvents, while large amounts of acids and bases were used, making the recycling of cellulose solvents difficult. It is worth noting that Swatoski *et al.* found that room temperature ionic liquids (RTILs) could efficiently dissolve cellulose, which opened up a new way for the development of cellulose dissolution and modification in this new solvent system.<sup>17</sup> RTILs, which are regarded as intrinsically “green” due to their negligible vapor pressure, have attracted great attention owing to their good thermal stability, high conductivity, low melting point and wide electrochemical window.<sup>18,19</sup>

In this work, 1-butyl-3-methylimidazolium ([Bmim]Cl) ionic liquid was used as solvent for the homogeneous modification of cellulose to prepare a cellulose-based adsorbent for Cr (VI) removal. The adsorbent was synthesized by chemical induced grafting copolymerization of styrene onto cellulose substrates, followed by chloroacetylation, amination and protonation processes. The shape and size of adsorbents can be easily adjusted according to the requirements of wastewater treatment. Meanwhile, the influencing factors on the grafting yield (GY) and the adsorption kinetics of Cr (VI) were systematically investigated.

## EXPERIMENTAL

### Materials

Microcrystalline cellulose (MCC) with a degree of polymerization of 215~240 and styrene (St) monomer were obtained from Shanghai Kefeng Chemical Reagents Co. Ltd. 1-Butyl-3-methylimidazolium ([Bmim]Cl) (>99%) was purchased from Lanzhou Institute of Chemical Physics (Lanzhou, China) and the water content was tested to be less than 0.9% by Karl-Fischer titration. Dimethyl sulfoxide (DMSO) and methylene-bis-acrylamide (MBA) were provided by Aladdin Industrial Corporation. Ammonium sulfate ((NH<sub>4</sub>)<sub>2</sub>S<sub>2</sub>O<sub>8</sub>) was obtained from Tianjin Chemical Reagent Co., Ltd. Other chemicals were analytical reagents and used as received.

### Synthesis of cellulose-g-PS

First, MCC was dispersed into [Bmim]Cl ionic liquid (*ca.* 5 g MCC/45 g [Bmim]Cl) and stirred for 24 h at 80 °C. The obtained limpid solution was diluted by adding DMSO (50 g). Then, (NH<sub>4</sub>)<sub>2</sub>S<sub>2</sub>O<sub>8</sub> was added as a chemical initiator at 60 °C and the obtained solution

was stirred for 20 min under nitrogen atmosphere, and to it St monomer and MBA cross-linking agent were added. All the conditions were kept unchanged until the end of the grafting reaction. After grafting, the solution was divided into two parts: the first part was modified by chloroacetylation, while the second part was used to calculate the grafting yield (GY). The procedures were as follows: after grafting, the obtained solution was transferred to culture dishes to form a membrane, which was washed with ethanol to regenerate cellulose; the regenerated cellulose membrane was covered by filter paper and washed in a Soxhlet extractor for 24 h in order to remove the homopolymer, the unreacted monomer and [Bmim]Cl. The obtained copolymers of cellulose and styrene, named as cellulose-*g*-PS, were finally dried in a vacuum drier at 70 °C until a constant weight was reached. The grafting yield, GY, was determined as follows:

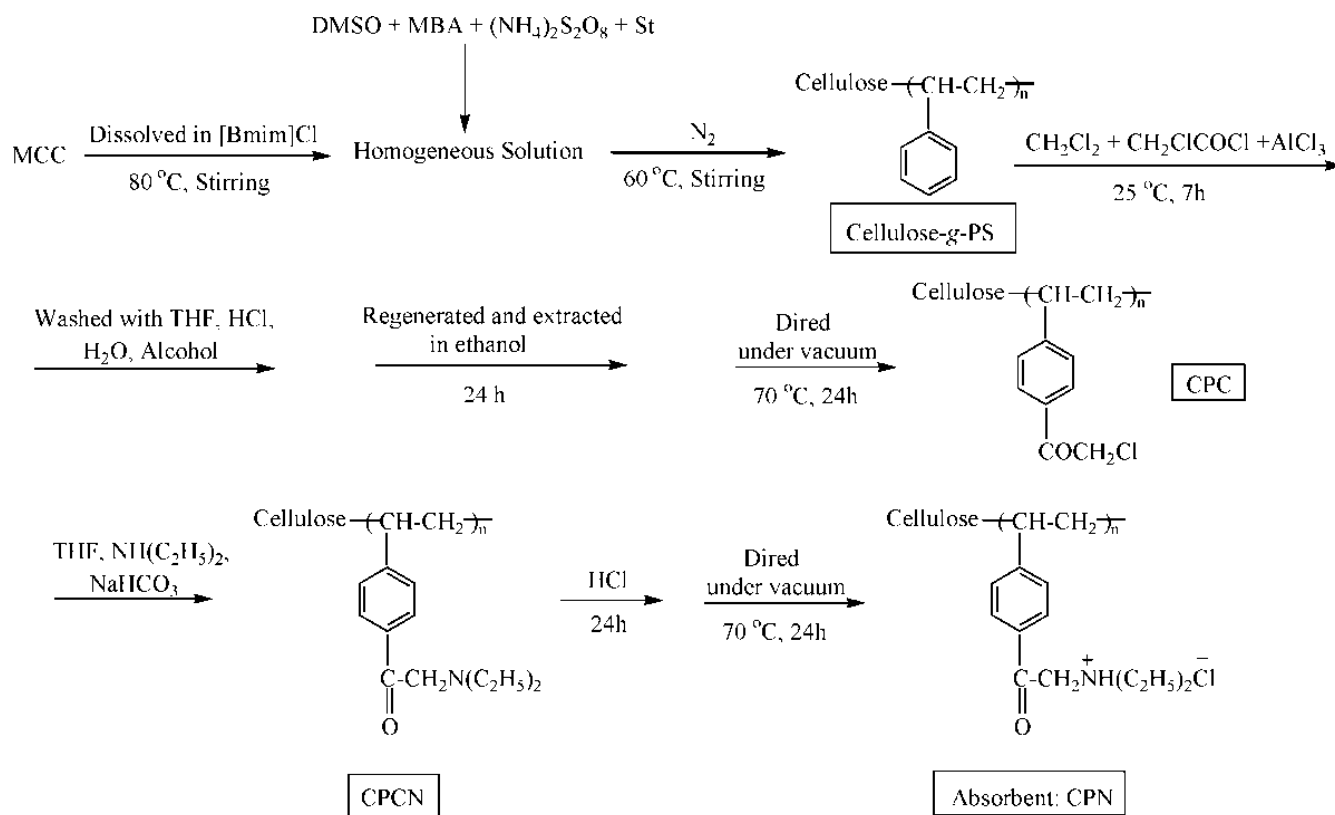
$$GY(\%) = \frac{W_1 - W_0}{W_0} \quad (1)$$

where  $W_0$  is the weight of MCC,  $W_1$  is the weight of cellulose-*g*-PS.

#### Preparation of the adsorbent

To cellulose-*g*-PS (5.0798 g),  $\text{CH}_2\text{Cl}_2$  (50 ml),  $\text{CH}_2\text{ClCOCl}$  (5.5140 g) and  $\text{AlCl}_3$  (12.6744 g) were

added in sequence. After a 7 h reaction at room temperature, the resulting product was first washed with THF, HCl, deionized water and methanol, and then extracted in a Soxhlet extractor for 24 h with ethanol. The as-prepared product was dried in a vacuum drier at 70 °C for 24 h and noted as chloroacetylation product (CPC). Subsequently, CPC (2.3160 g) was swelled in THF and, to it,  $\text{NH}(\text{C}_2\text{H}_5)_2$  (10.5541 g) and  $\text{NaHCO}_3$  (0.9353 g) were added. As the reaction continued, the color of the product changed from white to yellow. The amination product (CPCN) was then obtained by washing with deionized water. After the previous reactions, the solution was cast onto a glass plate and then immediately coagulated in ethanol in order to obtain a regenerated cellulose film with a thickness of about 0.50 mm.<sup>20</sup> In addition, the spherical cellulose adsorbent can also be obtained through the water-in-oil suspension technique. Thus, the shape and size of the adsorbents can be easily adjusted according to the requirements of wastewater treatment. Finally, CPCN was stirred in HCl (1 mol.L<sup>-1</sup>) at room temperature, washed with deionized water and dried in a vacuum drier at 70 °C for 24 h to get the target CPN adsorbent. The synthetic routes leading to the preparation of the CPN adsorbent are summarized in Scheme 1.



Scheme 1: Synthesis routes of CPN adsorbent in [Bmim]Cl ionic liquid

### Characterization of CPN

Micro-FTIR spectra of original MCC, regenerated cellulose, cellulose-*g*-PS, CPC and CPN were recorded on a Nicolet (Magna-IR 750) spectrometer within the wavenumber range of 4000–600  $\text{cm}^{-1}$ . AFM-IR measurements were carried out by depositing the adsorbent onto a ZnSe prism (transparent in the mid-IR). The deposit was observed by a nanoIRTM (Anasys Instruments), an AFM-IR system that combines AFM with a pulsed infrared OPO laser to perform spectromicroscopy. The morphologies of the samples before and after grafting were observed by SEM (HITACHI S-4300) and all the samples were gold sputtered. The thermal stability and composition analysis were performed on a thermogravimetric analysis instrument TGA Q600 under a nitrogen flow of 40  $\text{mL min}^{-1}$ . The temperature ranged from 30 to 700  $^{\circ}\text{C}$  at a heating rate of 15  $^{\circ}\text{C min}^{-1}$ .

### Adsorption capacity of Cr (VI)

Stock Cr (VI) solutions were prepared by using the procedure already reported.<sup>4</sup> A certain amount of HCl (0.02  $\text{mol L}^{-1}$ ) was added to stabilize Cr (VI) ions in the stock solution, which was subsequently diluted with deionized water to obtain the desired concentrations. The concentration of Cr (VI) was determined by UV-Vis absorption spectrophotometry at 258 nm.<sup>21,22</sup> The pH value of the solution was adjusted with HCl (1  $\text{mol L}^{-1}$ ) or NaOH (1  $\text{mol L}^{-1}$ ) and measured by a pH-meter (PHSJ-3F).

The adsorption of Cr (VI) ions was studied kinetically in a 50 mL solution containing 35  $\text{mg L}^{-1}$  Cr (VI), to which 20 mg of CPN adsorbent was added. All the solutions were covered and kept in an incubator at a constant temperature of 25  $^{\circ}\text{C}$  for different time intervals. The Cr (VI) uptake ( $q$ ) was calculated as follows:

$$q = (c_0 - c_t) \times V / m \quad (2)$$

where  $C_0$  and  $C_t$  ( $\text{mg L}^{-1}$ ) are the concentrations of Cr (VI) before and after adsorption, respectively;  $V$  (mL) is the volume of the Cr (VI) solution and  $m$  (mg) is the weight of the CPN adsorbent.

## RESULTS AND DISCUSSION

### Preparation of the CPN adsorbent

The influences of monomer and initiator concentrations, reaction time and reaction temperature on the grafting yield (GY) were studied in detail and shown in Figure 1.

From Figure 1a, it is clear that GY goes up and reaches a plateau as the concentration of the monomer increases. The results obtained can be reasonably explained by considering the fact that the total amount of reactive radicals formed on the cellulose substrates increased with the increase of the St monomer concentration.

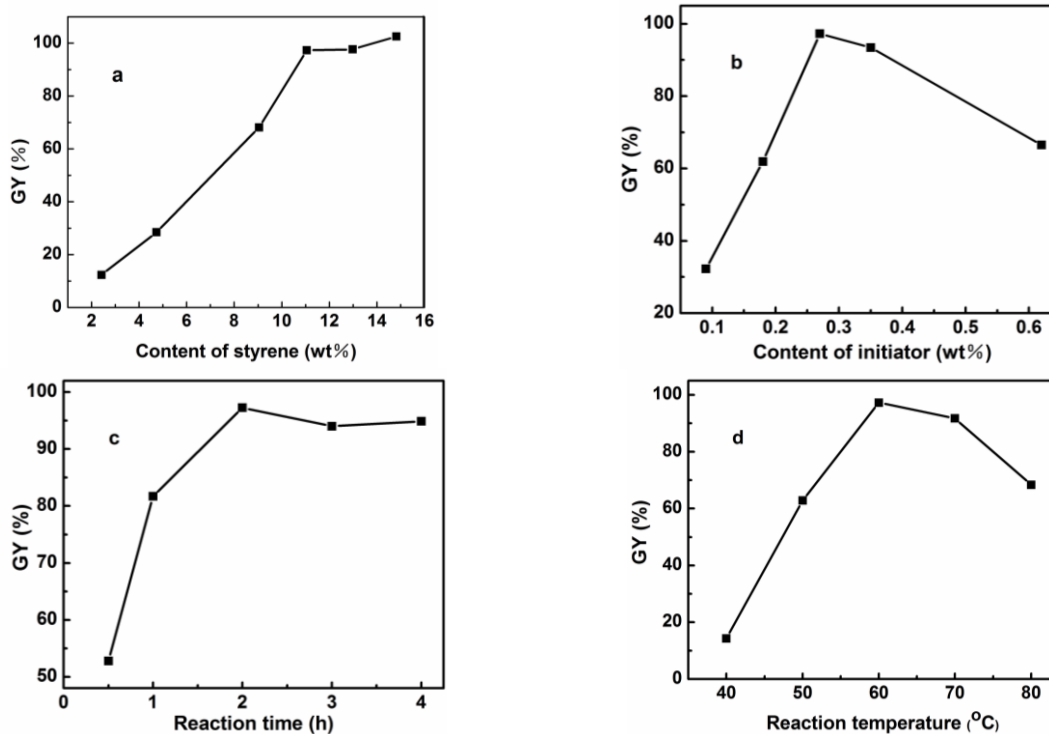


Figure 1: Influence of concentration of St monomer (a) and chemical initiator ( $\text{NH}_4$ )<sub>2</sub>S<sub>2</sub>O<sub>8</sub> (b), as well as reaction time (c) and reaction temperature (d) on GY

Nevertheless, the St monomer induces copolymerization rather than grafting as its content exceeds 11.1 wt%. Therefore, the appropriate mass percentage of the St monomer was fixed at 11.1 wt%. Figure 1b shows that GY increases as the concentration of the initiator rises and decreases when the amount of  $(\text{NH}_4)_2\text{S}_2\text{O}_8$  is over 0.3 wt%. Evidently, more reactive radicals are produced as the content of  $(\text{NH}_4)_2\text{S}_2\text{O}_8$  grows up, favoring the reaction between MCC and the St monomer, and leading to an increased GY. However, an excess in  $(\text{NH}_4)_2\text{S}_2\text{O}_8$  also promotes homopolymerization of the St monomer, leading to the further decrease of GY. As a result, the mass percentage of the  $(\text{NH}_4)_2\text{S}_2\text{O}_8$  initiator was chosen as 0.3 wt%.

The effects of reaction time and reaction temperature on the value of GY are presented in Figure 1c and 1d, respectively. When considering the reaction time, it is found that the GY value first increases, then remains almost constant after 2 h, indicating complete grafting of the St monomer. As a result, the optimal reaction time was found to be 2 h. Also, as observed in Figure 1c, the most suitable reaction temperature was found to be 60 °C. This could be explained by the fact that with an increase in reaction temperature, more reactive radicals are generated, leading to an increase in GY. Nevertheless, when the temperature becomes too high (higher than 60 °C here), it induces an increase in the rates of chain termination, chain transfer and homopolymerization reaction, leading to the decrease of GY.<sup>23</sup>

According to the results above, the preparation of the CPN adsorbent was carried out for 2 h at 60 °C with St monomer at a mass percentage of 11.1 wt% and with  $(\text{NH}_4)_2\text{S}_2\text{O}_8$  initiator at a mass percentage of 0.3 wt%. For comparison and further characterizations, the products with a calculated GY of 68.1% were selected.

### Characterization of CPN

In order to confirm the successful grafting of St and to study its effect on the thermal stability, the original MCC, regenerated cellulose, cellulose-*g*-PS (GY=68.1%), CPC and CPN adsorbent were analyzed by micro-FTIR and TGA.

Figure 2 presents the micro-FTIR spectra of all the samples. The spectra of the original MCC (Fig. 2a) and regenerated cellulose (Fig. 2b) are similar and the following characteristic bands are

observed: a large band between 3500~3300  $\text{cm}^{-1}$  corresponding to the stretching vibration of OH groups; a small band between 2900~2700  $\text{cm}^{-1}$  owing to  $-\text{CH}_2$  groups; characteristic bands at 1160 arising from C–O–C of glucosidic units.<sup>24</sup> Grafting of styrene is highlighted by the characteristic bands of the aromatic ring at 1490 and 1600  $\text{cm}^{-1}$ , which are attributed to C=C in-plane stretching vibration. The sharp peaks at 698 and 760  $\text{cm}^{-1}$  of cellulose-*g*-PS (Fig. 2c) are assigned to aromatic C-H deformation of the substituted benzene ring. The new band at 3025  $\text{cm}^{-1}$  is ascribed to =C-H stretching vibration of the aromatic ring.<sup>25</sup> The stretching vibration of carbonyl (C=O) of CPC is located at 1750  $\text{cm}^{-1}$  (Fig. 2d), indicating that the chloroacetyl groups have been attached to the original MCC.<sup>26</sup> In Figure 2e, the C=O band of CPN at 1750  $\text{cm}^{-1}$  is due to the substitution of chloroacetyl groups by amination. Therefore, the results of micro-FTIR spectra prove that the CPN adsorbent was successfully synthesized.

In order to observe the surface morphology of the CPN adsorbent and also to check the distribution of functional groups in it, the as-prepared adsorbent was characterized by AFM-IR nanospectroscopy. AFM was used in the contact mode. The combination of AFM and IR laser pulse was applied to draw the chemical maps of the characteristic bands of the functional groups at different wavenumbers.<sup>27</sup> The results are shown in Figure 3.

According to the topographic image recorded by AFM in Figure 3a, the CPN adsorbent exhibits big globular aggregates (~2.5  $\mu\text{m}$ ) made up of smaller, more or less spherical particles (marked by arrows). The chemical maps of the CPN adsorbent were recorded in parallel by tuning the IR source at 1160, 1490 and 1735  $\text{cm}^{-1}$ , which correspond to original MCC, in-plane stretching vibration of aromatic C=C and C=O groups, respectively.

As observed in Figure 3b, the chemical map obtained with the characteristic band of original MCC fits very well with the topography of the CPN adsorbent. The red areas indicate that a high amount of MCC exists in the corresponding regions. Therefore, it is clear that the CPN adsorbent mostly contains MCC substrate. Similarly, the chemical maps recorded at the characteristic wavenumbers of C=C and C=O groups show quite similar features as that of original MCC. These results further demonstrate

successful grafting of styrene and quantitative chloroacetylation onto original MCC. They also prove the homogeneous distribution of C=C and C=O groups in the CPN adsorbent. The AFM-IR

results are in good agreement with those of micro-FTIR and further characterize the morphology of the CPN adsorbent, as well as its composition.

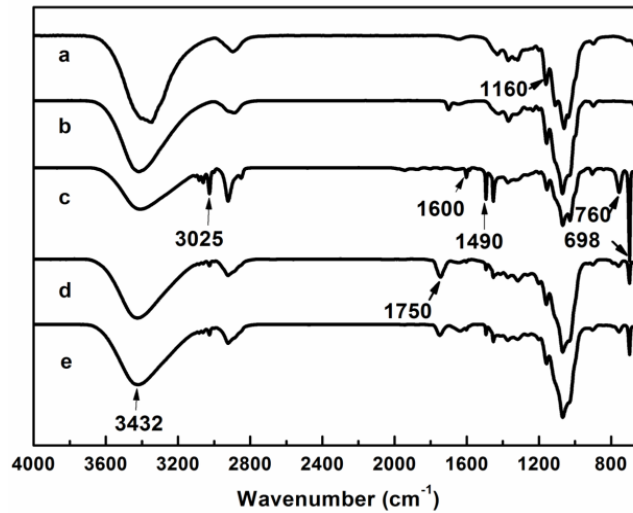


Figure 2: FT-IR spectra of original MCC (a), regenerated cellulose (b), cellulose-g-PS (GY=68.1%) (c), CPC (d) and CPN (e)

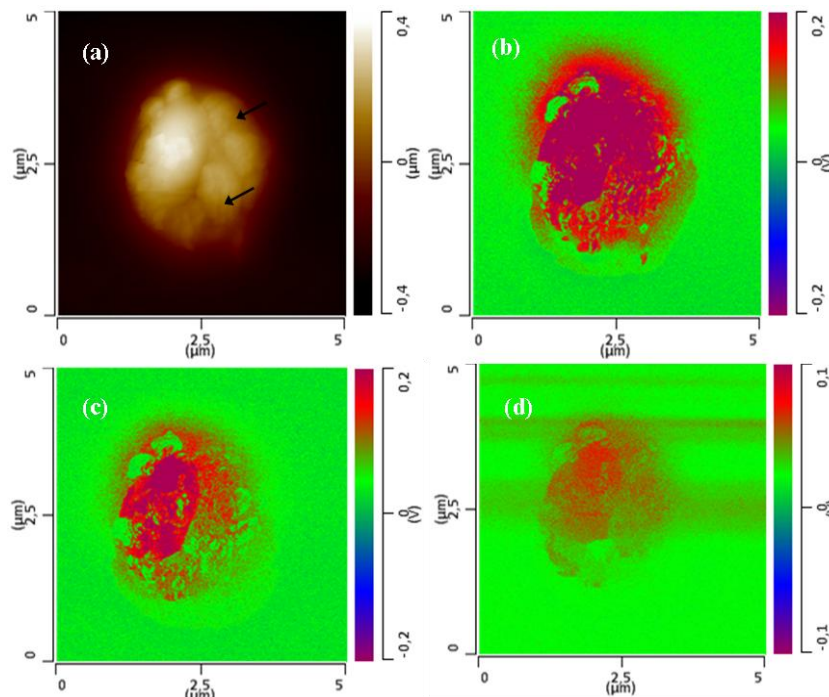


Figure 3: Topographic image of CPN adsorbent (a) and chemical maps of CPN adsorbent obtained at wavenumbers of 1160  $\text{cm}^{-1}$  (b), 1490  $\text{cm}^{-1}$  (c) and 1735  $\text{cm}^{-1}$  (d)

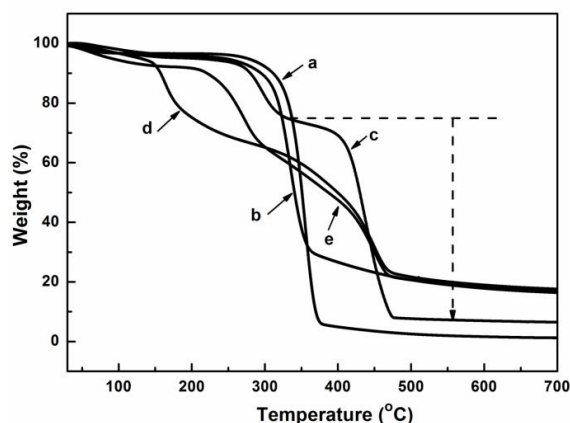


Figure 4: TGA curves of original MCC (a), regenerated cellulose (b), cellulose-g-PS (GY=68.1%) (c), CPC (d) and CPN (e)

In order to study the thermal stability and to further determine the amount of grafting groups onto the cellulose substrate, the TGA curves of all the samples were recorded as illustrated in Figure 4.

All the samples have a small weight loss below 120 °C, corresponding to the loss of physically adsorbed water from the samples. Compared with original MCC (Fig. 4a), the regenerated cellulose (Fig. 4b) exhibits a lower onset temperature of decomposition, but gives a higher char yield after pyrolysis. In addition, the residual of original MCC is 1.6% at 600 °C, whereas 17.8% remains from regenerated cellulose at the same temperature due to the formation of nonvolatile carbonaceous material.<sup>17</sup> Cellulose-g-PS (Fig. 4c) undergoes two-step degradation, in which the degradation of MCC occurs first and then the decomposition of grafted styrene, resulting in a weight loss of 66.6%, which is close to the calculated GY (68.1%). Moreover, the residual of cellulose-g-PS decreases, compared with that of regenerated cellulose, implying covalent attachment of the polystyrene chains to original MCC.<sup>28</sup>

The TGA curves of CPC (Fig. 4d) and CPN (Fig. 4e) show that chloroacetylation and amination of cellulose have no effect on the thermal stability of cellulose, which is in agreement with other reported results.<sup>29</sup> However, it is found that the decomposition temperature ( $T_d$ ) of all the cellulose derivatives is lower than that of original MCC. This decrease of  $T_d$  may arise from the decreasing crystalline degree of MCC in all the cellulose derivatives.<sup>30</sup> Therefore, TGA analysis agrees well with the calculated GY of St and proves that functionalization has no

effect on the thermal stability of original MCC, but lowers its crystalline degree.

The morphology of regenerated cellulose and cellulose-g-PS with different GY (68.1% and 97.3%) were observed by SEM microscopy and typical images are shown in Figure 5. It is clear that the regenerated cellulose (Fig. 5a) appears as smooth surface while cellulose-g-PS (Fig. 5b and 5c) appears as rough nano-scaled particles. This morphological difference indicates the existence of homopolymer of St in regenerated cellulose and complete elimination in cellulose-g-PS after washing. As the GY increases, the roughness increases arising from the enlarged particle size. Thus, the observed morphology of cellulose-g-PS by SEM is similar to that of the topography recorded by AFM and the increased particle size roughens the surface of cellulose-g-PS.

## Adsorption of Cr (VI)

### Adsorption kinetics

The effect of contact time on the adsorption of Cr (VI) by the CPN adsorbent was studied and shown in Figure 6.

Obviously, the removal rate of Cr (VI) onto the CPN adsorbent rose rapidly in the initial stage, until it reached adsorption equilibrium after 30 min. The adsorption kinetics can be analyzed using pseudo-first-order and pseudo-second-order kinetic models as follows:<sup>31</sup>

$$\text{Pseudo-first-order: } \ln(q_e - q_t) = \ln q_e - k_1 t \quad (3)$$

$$\text{Pseudo-second-order: } \frac{t}{q_t} = \frac{1}{k_2 q_e^2} + \frac{t}{q_e} \quad (4)$$

where  $q_e$  and  $q_t$  are the amounts of Cr (VI) sorption ( $\text{mg g}^{-1}$ ) at equilibrium and at the contact

time  $t$  (min);  $k_1$  and  $k_2$  are the corresponding kinetic rate constants.

The fitting results according to the two different models are summarized in Table 1. According to the correlation coefficient ( $R^2$ ), the

adsorption of Cr (VI) by the CPN adsorbent obeys the pseudo-second-order kinetics ( $R^2=0.999$ ), which suggests that chemical interaction is involved in the adsorption of Cr (VI) onto the CPN adsorbent.<sup>32</sup>

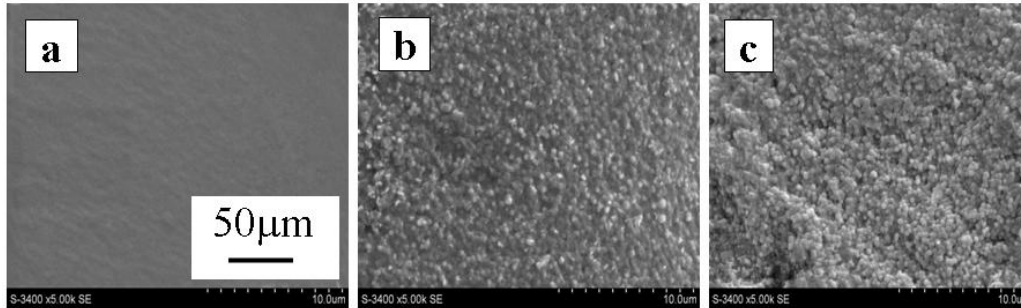


Figure 5: SEM images of regenerated cellulose (a), cellulose-g-PS with GY of 68.1% (b) and 97.3% (c)

Table 1  
Kinetic parameters of model fitting for adsorption of Cr (VI) by CPN adsorbent

Adsorbent	Pseudo-first-order			Pseudo-second-order		
	$k_1$ ( $\text{min}^{-1}$ )	$q_e$ ( $\text{mg g}^{-1}$ )	$R^2$	$k_2$ ( $\text{g mg}^{-1} \text{min}^{-1}$ )	$q_e$ ( $\text{mg g}^{-1}$ )	$R^2$
CPN	2.333	20.986	0.877	0.0283	20.670	0.999

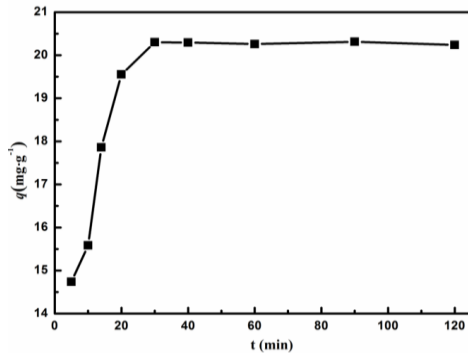


Figure 6: Adsorption kinetics of Cr (VI) by CPN adsorbent in 50 mL of solution (Cr (VI):  $35 \text{ mg L}^{-1}$ )

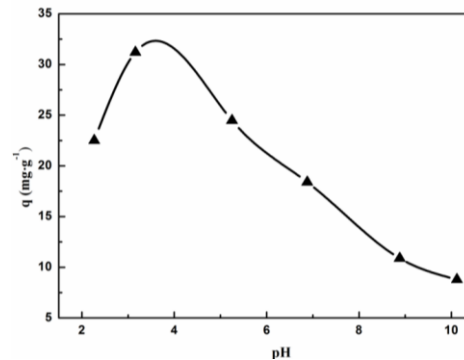


Figure 7: Effect of pH on Cr (VI) uptake, (Cr (VI) concentration:  $35 \text{ mg L}^{-1}$ ; adsorbent feed:  $0.7 \text{ g L}^{-1}$ ; stirring time: 40 min;  $V$ : 50 mL)

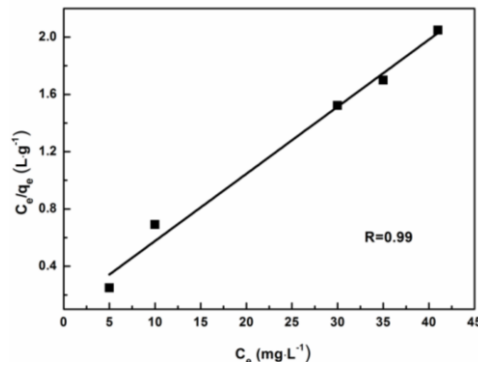


Figure 8: Langmuir isotherm plot of Cr (VI) adsorption by CPN adsorbent

### Effect of pH

As pH influences both the surface charge of the adsorbent and the existing form of Cr (VI), it is necessary to study the Cr (VI) uptake at different pH values. The results are shown in Figure 7.

It is clear that the CPN adsorbent can work under a wide range of pH values, from 2 to 10. As the pH increases from 2 to 4, the Cr (VI) uptake increases from 22.5 to 31.2 mg g<sup>-1</sup>. It is well known that Cr (VI) can be stabilized as Cr<sub>2</sub>O<sub>7</sub><sup>2-</sup>, HCrO<sub>4</sub><sup>-</sup>, H<sub>2</sub>Cr<sub>2</sub>O<sub>7</sub> and CrO<sub>4</sub><sup>2-</sup> complexes and that their relative abundance depends on the pH and on Cr (VI) concentration. When pH is lower than 1, H<sub>2</sub>CrO<sub>4</sub> is predominant, while HCrO<sub>4</sub><sup>-</sup> predominates in the pH range of 1 to 6.<sup>4</sup> Also, when the pH is lower than 7, the functional amino groups of the CPN adsorbent are protonated into -NH<sub>3</sub><sup>+</sup>, which constitute, thanks to electrostatic interactions, efficient adsorption centers towards Cr (VI) complexes. However, the Cr (VI) uptake decreases obviously when the pH is higher than 7. Indeed, in alkaline solutions, Cr (VI) mainly exists as CrO<sub>4</sub><sup>2-</sup> anions, while the amount of positively charged adsorption centers is reduced, resulting from the competition of HO<sup>-</sup> and the deprotonation of the -NH<sup>+</sup>(C<sub>2</sub>H<sub>5</sub>)<sub>2</sub> groups, leading to lower adsorption efficiency of the CPN adsorbent. Thus, the optimal pH value for Cr (VI) uptake is in the range of 2 to 7.

### Isotherm of Cr (VI) adsorption

The Langmuir isotherm model was applied to establish the relationship between Cr (VI) uptake and equilibrium concentration in the aqueous solution. The data were collected and analyzed by the Langmuir isotherm model described in Equation (5):

$$\frac{C_e}{q_e} = \frac{C_e}{q_m} + \frac{1}{K_L q_m} \quad (5)$$

where  $C_e$  is the equilibrium concentration of Cr (VI) (mg L<sup>-1</sup>) and  $q_e$  is the amount of Cr (VI) adsorbed by per gram of adsorbent (mg g<sup>-1</sup>) at equilibrium, respectively.  $q_m$  and  $K_L$  are Langmuir constants related to the adsorption capacity (mg g<sup>-1</sup>) and the adsorption energy (L g<sup>-1</sup>), respectively.  $q_m$  and  $K_L$  are calculated according to the slope and the intercept of  $C_e/q_e$  versus  $C_e$ , respectively. The Langmuir isotherm plot for Cr (VI) adsorption using the CPN adsorbent is plotted in Figure 8.

The linear relation coefficient,  $R^2$ , is found to be 0.99, revealing that the adsorption of Cr (VI) by the CPN adsorbent fits well with the Langmuir model. From the linear relationship, the isotherm constants  $q_m$  and  $K_L$  are determined as 32.5 mg g<sup>-1</sup> and 0.285 L g<sup>-1</sup>, respectively. It has been reported that the maximal uptake of Cr (VI) by a variety of modified and unmodified biosorbents ranges from 0.15 to 256 mg g<sup>-1</sup>.<sup>33,34</sup> Compared with the reported adsorption capacity of Cr (VI) uptake, the CPN adsorbent has a moderate adsorption capacity towards Cr (VI). Besides, the present CPN adsorbent could also adsorb other heavy metal ions, such as Cu (II) ions. Therefore, the CPN adsorbent can have a potential application as adsorption material, which will be investigated in our further research work.

### CONCLUSION

A novel amino-functionalized cellulose adsorbent was prepared in an ionic liquid homogeneous system by grafting a styrene monomer onto an MCC substrate, followed by acetylation, amination and protonation processes. Micro-FTIR and AFM-IR characterizations confirmed successful grafting and copolymerization of styrene onto the MCC substrate, along with homogenous distribution of functional groups. The GY can be controlled by changing the concentrations of the monomer and initiator, and by adjusting the reaction time and the reaction temperature. Adsorption of Cr (VI) from an aqueous solution by the resulting CPN adsorbent was tested and adsorption equilibrium was reached within 30 min. As highlighted, the adsorption capacity strongly depends on the pH value and the optimal pH was found in the range of 2 to 7. As demonstrated, Cr (VI) adsorption onto the CPN adsorbent follows pseudo-second-order kinetics, suggesting that the adsorption corresponds to a process of ion exchange. The adsorption isotherm indicates that the adsorption behavior of CPN fits with the Langmuir model, with an optimal Cr (VI) uptake of 32.5 mg g<sup>-1</sup>. Definitely, this work provides a new cellulose-based adsorbent for Cr (VI) removal from wastewater and gives us a glimpse of future promising applications.

**ACKNOWLEDGEMENT:** This work was supported by the Natural Science Foundation of Inner Mongolia (2017MS0220) and the National

Natural Science Foundation of China (NNSFC, Project No. 21463016).

## REFERENCES

- <sup>1</sup> T. Hajeeth, K. Vijayalakshmi, T. Gomathi, P. N. Sudha and S. Anbalagan, *Compos. Interfaces*, **21**, 75 (2014).
- <sup>2</sup> D. W. O'Connell, C. Birkinshaw and T. F. O'Dwyer, *Bioresour. Technol.*, **99**, 6709 (2008).
- <sup>3</sup> Y. G. El-Reash, M. Otto, I. M. Kenawy and A. M. Ouf, *Int. J. Biol. Macromol.*, **49**, 513 (2011).
- <sup>4</sup> J. Y. Qiu, Z. Y. Wang, H. B. Li, L. Xu, J. Peng et al., *J. Hazard. Mater.*, **166**, 270 (2009).
- <sup>5</sup> B. Qiu, C. X. Xu, D. Z. Sun, Q. Wang, H. D. Gu et al., *Appl. Surf. Sci.*, **334**, 7 (2015).
- <sup>6</sup> Z. H. Ai, Y. Cheng, L. Z. Zhang and J. R. Qiu, *Environ. Sci. Technol.*, **42**, 6955 (2008).
- <sup>7</sup> D. H. Camacho, S. P. Gerongay and J. P. Macalinao, *Cellulose Chem. Technol.*, **47**, 125 (2013).
- <sup>8</sup> J. H. Zu, L. Tong, X. W. Liu and G. S. Sun, *J. Appl. Polym. Sci.*, **107**, 1252 (2008).
- <sup>9</sup> S. Asai, K. Watanabe, T. Sugo and K. Saito, *J. Chem. Thermodyn.*, **1094**, 158 (2005).
- <sup>10</sup> D. Klemm, B. Heublein, H. P. Fink and A. Bohn, *Angew. Chem.-Int. Ed.*, **44**, 3358 (2005).
- <sup>11</sup> T. Sathvika, Manasi, V. Rajesh and N. Rajesh, *Chem. Eng. J.*, **279**, 38 (2015).
- <sup>12</sup> T. Hajeeth, P. N. Sudha and K. V. Vijayalakshmi, *Cellulose Chem. Technol.*, **49**, 891 (2015).
- <sup>13</sup> R. R. Navarro, K. Sumi, N. Fujii and M. Matsumura, *Water Res.*, **30**, 2488 (1996).
- <sup>14</sup> Z. M. Wang, L. Li, K. J. Xiao and J. Y. Wu, *Bioresour. Technol.*, **100**, 1687 (2009).
- <sup>15</sup> Q. Xu, J. F. Kennedy and L. J. Liu, *Carbohydr. Polym.*, **72**, 113 (2008).
- <sup>16</sup> X. T. Sun, L. R. Yang, Q. Li, J. M. Zhao, X. P. Li et al., *Chem. Eng. J.*, **241**, 175 (2014).
- <sup>17</sup> R. P. Swatloski, S. K. Spear, J. D. Holbrey and R. D. Rogers, *J. Am. Chem. Soc.*, **124**, 4974 (2002).
- <sup>18</sup> J. Dupont, C. S. Consorti and J. Spencer, *J. Braz. Chem. Soc.*, **11**, 337 (2000).
- <sup>19</sup> R. Bini, C. Chiappe, C. Duce, A. Micheli, R. Solaro et al., *Green Chem.*, **10**, 314 (2008).
- <sup>20</sup> Y. Hao, J. Peng, J. Q. Li, M. L. Zhai and G. S. Wei, *Carbohydr. Polym.*, **77**, 779 (2009).
- <sup>21</sup> F. Compere, G. Porel and F. Delay, *J. Contam. Hydrol.*, **49**, 1 (2001).
- <sup>22</sup> M. Noroozifar and M. Khorasani-Motlagh, *Anal. Sci.*, **19**, 705 (2003).
- <sup>23</sup> K. C. Gupta and K. Khandekar, *Biomacromolecules*, **4**, 758 (2003).
- <sup>24</sup> D. M. Suflet, G. C. Chitanu and V. I. Popa, *React. Funct. Polym.*, **66**, 1240 (2006).
- <sup>25</sup> Z. B. Zhang and C. L. McCormick, *J. Appl. Polym. Sci.*, **66**, 307 (1997).
- <sup>26</sup> C. X. Lin, H. Y. Zhan, M. H. Liu, S. Y. Fu and L. A. Lucia, *Carbohydr. Polym.*, **78**, 432 (2009).
- <sup>27</sup> Z. Cui, C. Coletta, A. Dazzi, P. Lefrancois, M. Gervais et al., *Langmuir*, **30**, 14086 (2014).
- <sup>28</sup> D. Roy, J. T. Guthrie and S. Perrier, *Macromolecules*, **38**, 10363 (2005).
- <sup>29</sup> S. R. Labafzadeh, K. Vyavaharkar, J. S. Kavakka, W. T. Alistair and L. Kilpelainen, *Carbohydr. Polym.*, **116**, 60 (2015).
- <sup>30</sup> C. Y. Yin, J. B. Li, Q. Xu, Q. Peng, Y. B. Liu et al., *Carbohydr. Polym.*, **67**, 147 (2007).
- <sup>31</sup> T. S. Anirudhan and P. Senan, *Chem. Eng. J.*, **168**, 678 (2011).
- <sup>32</sup> L. Zhao, J. Sun, Y. Zhao, L. Xu and M. L. Zhai, *Chem. Eng. J.*, **170**, 162 (2011).
- <sup>33</sup> C. H. Weng, Y. C. Sharma and S. H. Chu, *J. Hazard. Mater.*, **155**, 65 (2008).
- <sup>34</sup> M. Owlad, M. K. Aroua, W. A. Daud and S. Baroutian, *Water Air Soil Pollut.*, **200**, 59 (2009).